J. Plasma Physics (2005), *vol.* 71, *part* 1, *pp.* 11–21.
DOI: 10.1017/S0022377804002946 Printed in the United Kingdom

Coherence–incoherence transition in nonlinear wave interactions

M. FRICHEMBRUDER, R. PAKTER and F. B. RIZZATO†

Instituto de Física, Universidade Federal do Rio Grande do Sul, Caixa Postal 15051, 91501-970 Porto Alegre, Rio Grande do Sul, Brasil
(rizzato@if.ufrgs.br)

(Received 25 July 2003, revised 20 January 2004 and accepted 2 February 2004)

Abstract. In this paper we analyze the transition from coherent to incoherent wave dynamics in a broad-band triplet interaction, where, in contrast to previous models, wave vector selection rules are imposed on the nonlinear terms of the governing equations. As a general rule, nonlinear terms induce coherence via a phase-locking process. However, wave vector spread also results from nonlinearity and can affect coherence when resonant modes are excited.

1. Introduction

Nonlinear wave dynamics can be frequently modeled by the interaction of a few monochromatic modes (Weiland and Wilhelmsson 1977; Thornhill and ter Haar 1978; Shukla et al. 1986). In many cases the dynamics involves three higher-amplitude modes in which case one refers to the model as the triplet wave interaction. Triplet interaction is one of the most significant forms of wave interaction, presenting the most prominent nonlinear features in wave systems. It comes in several versions, and the version we examine here is the conservative regime. A large variety of situations can be described by the conservative triplet interaction as, for instance, decay instabilities in laser–plasma interactions, three mode interaction in nonlinear optical systems and other nonlinear cases (Shukla et al. 1986; Kivshar and Malomed 1989; Chian and Alves 1988; Gratton et al. 1997; Frichembruder et al. 2000). The governing equations of the classic pure triplet can be fully integrated and the modes can be shown to undergo a periodical energy exchange among themselves (Weiland and Wilhelmsson 1977). Now, a question analyzed by a number of researchers concerns the preservation of this kind of periodic behavior when each of the three single modes of the classic picture is replaced with a narrow comb of many modes (Weiland and Wilhelmsson 1977; Martins and Mendonça 1988; Robinson and Drysdale 1996; Drysdale and Robinson 2002; Rizzato et al. 2003). If the multitude of modes in each comb acts coherently as a single mode, one can expect to see periodicity. Otherwise, when coherence is lost, more complicated behaviors are likely. The former situation is known as the fixed-phase regime of the nonlinear interaction and the latter is known as the random-phase regime. Given a physical problem, one generally makes an *a priori* choice based on the environmental conditions and exclusively uses either the fixed-phase or the random-phase approach. Our interest here nevertheless is to examine the transition from

† Corresponding author, e-mail: rizzato@if.ufrgs.br. Fax: +55 513316-7286.

one regime to another based on a more microscopic view. A precise and detailed answer to the problem is involved. However, some clear analytical estimates and results are provided for the class of interaction where any mode j in one comb, say comb '1', interacts democratically with all modes l, m of the other two combs following a general rule $\dot{a_{1j}} \sim \sum_{l,m} a_{2l}a_{3m}$. Here the double summation over l and m is unrestricted and one arrives at well-defined rules relating the threshold field for the transition from coherence to incoherence, and the width of the combs. The basic result is that coherence is preserved as long as the wave amplitudes are large enough that they create a strong mean field trapping all modes in a phase-locking state (Robinson and Drysdale 1996; de Oliveira et al. 2002; Drysdale and Robinson 2002; Rizzato et al. 2003). On the other hand, if field amplitudes are small, phase-locking is absent and coherence is lost. In this case the interaction is best described in terms of random-phase approximations.

Unrestricted summation can be partly justified, and should be seen as an approximative approach, if spatial resolution is poor (Weiland and Wilhelmsson 1977). Then one can perform partial summations over subsets of microscopic modes to arrive at this type of nonlinear term. In the present work, we examine the problem without performing the summation over the subsets of microscopic modes. In other words, we keep our analysis more aligned with the spirit of conventional Fourier transforms adopting the more usual shape for the nonlinear terms $\dot{a_{1j}} \sim \sum'_{l,m} a_{2l}a_{3m}$, where the now primed summation obeys a selection rule of the general symbolic form $j = j(l, m)$. In addition to that, we allow for the gradual inclusion of modes as demanded by the dynamics; in previous works the number of modes of each comb is held fixed. This particular analysis of the coherence–incoherence transition has not been performed and generalizes the previous analysis based on unrestricted summations. The idea is to see if the transition maintains the overall properties. As a preview of our results, one can say that in general terms we shall see that the basic features detected previously can still be observed, although in a modified form.

The paper is organized as follows: in Sec. 2 we introduce the relevant governing equations, in Sec. 3 we make use of stationary-phase approximations to produce some estimates on the number of involved modes for a given field amplitude, in Sec. 4 we perform a series of numerical simulations to analyze dynamical evolution and the final saturated states of the interaction, and in Sec. 5 we conclude the work.

2. Governing equations

Given three combs of modes, '1', '2', and '3', the unrestricted version of the nonlinear interaction takes the form

$$i\dot{a_{1j}}(t) - (\Omega_1 + v_{g_1}\kappa_j)a_{1j} = \frac{1}{N}\sum_{l,m} a_{2l}a_{3m}, \tag{2.1}$$

$$i\dot{a_{2j}}(t) - (\Omega_2 + v_{g_2}\kappa_j)a_{2j} = \frac{1}{N}\sum_{l,m} a_{1l}a^*_{3m}, \tag{2.2}$$

$$i\dot{a_{3j}}(t) - (\Omega_3 + v_{g_3}\kappa_j)a_{3j} = \frac{1}{N}\sum_{l,m} a_{1l}a^*_{2m}, \tag{2.3}$$

with dots indicating time derivatives and with j, l, m as integers denoting any of the N modes within each comb (Martins and Mendonça 1988; Robinson and Drysdale 1996; de Oliveira et al. 2002). Note that in this unrestricted case, the summation is to be performed disjointedly over l and m. We introduce $\kappa_j \equiv -\Delta + (j-1)/(N-1)2\Delta$, so the average $\overline{\kappa_j} \equiv (1/N)\sum_j \kappa_j = 0$. Now if one discards nonlinear terms, $a_{p_j} \sim \exp(-i\Omega_{p_j} t)$ with $\Omega_{p_j} \equiv \Omega_p + v_{g_p}\kappa_j$ and $\overline{\Omega_{p_j}} = \Omega_p$ $(p = 1, 2, 3)$. Given all these facts, Ω_p can be thus seen as the central frequency of each comb and $v_{g_p}\kappa_j$ as a spectral quantity describing a narrow frequency broadening of width $2v_{g_p}\Delta$. v_{g_p} in fact scales the broadening of each comb.

We now undo the approximations leading to (2.1)–(2.3), transforming the nonlinear terms according to the rules:

$$(1/N)\sum_{l,m} a_{2l} a_{3m} \to \sum_{\kappa_l + \kappa_m = \kappa_j} a_{2l} a_{3m}, \tag{2.4}$$

$$(1/N)\sum_{l,m} a_{1l} a_{3m}^{*} \to \sum_{\kappa_l - \kappa_m = \kappa_j} a_{1l} a_{3m}^{*}, \tag{2.5}$$

$$(1/N)\sum_{l,m} a_{1l} a_{2m}^{*} \to \sum_{\kappa_l - \kappa_m = \kappa_j} a_{1l} a_{2m}^{*}. \tag{2.6}$$

In addition, we consider large enough values of N and Δ such that even modes not present in the original combs at $t = 0$ may be excited along the dynamics. With this model of interaction the nonlinear term can be seen as the usual Fourier transform of a local interaction, a feature we explore in the following. Let us first rewrite the governing equations in the final form

$$i\dot{a}_{1j}(t) - v_{g_1}\kappa_j a_{1j} = \sum_{\kappa_l + \kappa_m = \kappa_j} a_{2l} a_{3m}, \tag{2.7}$$

$$i\dot{a}_{2j}(t) - v_{g_2}\kappa_j a_{2j} = \sum_{\kappa_l - \kappa_m = \kappa_j} a_{1l} a_{3m}^{*}, \tag{2.8}$$

$$i\dot{a}_{3j}(t) - v_{g_3}\kappa_j a_{3j} = \sum_{\kappa_l - \kappa_m = \kappa_j} a_{1l} a_{2m}^{*}, \tag{2.9}$$

where the central frequency of each comb has been removed through the redefinitions $a_{p_j} \to a_{p_j} e^{-i\Omega_p t}$, and where the frequency matching condition $\Omega_1 = \Omega_2 + \Omega_3$ is chosen to enhance the interaction. Now we introduce the spatial representation of an arbitrary quantity g as $g(x,t) = \sum_j g_j(t) e^{i\kappa_j x}$ within a spatial region of length $L \equiv 2\pi/(2\Delta/N) = N\pi/\Delta$ to rewrite set (2.7)–(2.9) in its space–time form

$$i(\partial_t + v_{g_1}\partial_x)a_1 = a_2 a_3, \tag{2.10}$$

$$i(\partial_t + v_{g_2}\partial_x)a_2 = a_1 a_3^{*}, \tag{2.11}$$

$$i(\partial_t + v_{g_3}\partial_x)a_3 = a_1 a_2^{*}, \tag{2.12}$$

which is meaningful when the spectra a_{p_j} fall fast enough with κ_j. The set of equations (2.10)–(2.12) governs the nonlinear interaction of a triplet of waves where each mode is allowed to develop spatiotemporal modulations. The set may be used to describe three wave dynamics related to Langmuir and electromagnetic decays in plasmas (Wong and Quon 1975; Zakharov et al. 1985), three wave interaction in nonlinear optics (Ablowitz and Segur 1981), and several other three wave settings, whenever spatial localization is a relevant feature. The set (2.10)–(2.12) is known,

but the novelty here is that we use it to establish the boundaries between coherent and incoherent dynamics in the case where summations involving nonlinear terms obey selection rules imposed by proper Fourier transform as represented in (2.7)–(2.9). This sort of analysis has not been done before and we compare our results with those obtained when selection rules are relaxed, as in the set (2.1)–(2.3). The scale factors v_{g_p} can now be seen as group velocities, and their influence on the transition to incoherence is critical as we shall see below.

3. Case of equal group velocities and test mode calculations

We first investigate the case analyzed elsewhere (Robinson and Drysdale 1996) where equal group velocities are assumed: $v_{g_1} = v_{g_2} = v_{g_3} \equiv v_g$. This situation serves as the basis for our analysis, and can be physically realized in the dispersionless case of Alfvén waves, where two transverse Alfvén modes have the same group velocity (Sagdeev and Galeev 1969). In the Alfvén case the third mode moves with a different velocity (it is a longitudinal mode), but this velocity deviation is precisely the generic effect we intend to investigate in our next step. While in the unrestricted case one may have either coherent or incoherent dynamics for this setting, depending on the chosen field amplitudes, in the present restricted case the system behaves coherently as we shall now see. Indeed, if one looks at (2.10)–(2.12) with equal group velocities and introduces new variables according to $t \to t$, $x - v_g t \to x$, the set can be rewritten in the form

$$i\partial_t a_1 = a_2 a_3, \tag{3.1}$$

$$i\partial_t a_2 = a_1 a_3^*, \tag{3.2}$$

$$i\partial_t a_3 = a_1 a_2^*, \tag{3.3}$$

which is independent of spatial derivatives and the corresponding frequency broadenings. The set (3.1)–(3.3) not only represents the case of equal group velocities, but also serves as the basis of a perturbative calculation for more generic situations where group velocities differ slightly from each other. In this latter case, one regards (3.1)–(3.3) as generating unperturbed bulk solutions which shall drive the perturbed modes seen as test modes. If test modes keep close resemblance to their unperturbed counterpart, solutions of (3.1)–(3.3) may be expected to represent the dynamics well. Otherwise, the system behavior is expected to undergo considerable changes.

Now, in the absence of linear broadening one might suspect that coherence would be dominant. However, this is not at all guaranteed. The situation here contrasts largely with the unrestricted case (2.1)–(2.3) where the nonlinear term is exactly the same for all modes in one comb. In the present analysis, given the selection rules of all summations of (2.7)–(2.9), each mode is driven by a different subset of the modes contained in the other combs and this asymmetry gives no guarantee that all modes will vibrate synchronously. One must therefore verify whether or not coherence really sets in, in the absence of linear frequency broadening. If coherence is present in this situation, we can expect it to remain present even when a small broadening is included into the problem; transition to incoherence could be thus seen as resulting from the competition between linear broadening and nonlinear phase-locking, just as in previous studies (Robinson and Drysdale 1996; de Oliveira et al. 2002). Let us examine the issue.

We can invoke techniques of nonlinear wave analysis and separate each field in the set (3.1)–(3.3) in the form $a_p(x,t) \equiv \rho_p(x,t)\exp(i\phi_p(x,t))$. To simplify the analysis we look for steady-state solutions characterized by the condition $\dot{\rho}_p = 0$. This is not the more general solution, but it contains all the relevant ingredients we are seeking (Robinson and Drysdale 1996; de Oliveira et al. 2002). In addition, it represents reasonable experimental conditions where one looks for stationary interaction. The time independence of the amplitudes ρ_p is achieved when (Weiland and Wilhelmsson 1977):

$$\rho_2(x) = \rho_3(x) = \sqrt{2}\rho_1(x), \tag{3.4}$$

$$\phi_2(x,t) + \phi_3(x,t) - \phi_1(x,t) \equiv \Theta = 0. \tag{3.5}$$

There are similar fixed points like one at $\Theta = \pi$, but the results are equivalent to the $\Theta = 0$ case we scrutinize here. In any case, one sees that even at fixed points the phases ϕ are not time independent. As a matter of fact, the corresponding solutions in our study read

$$\phi_1(x,t) = -2\rho_1(x)t, \quad \phi_{(2,3)}(x,t) = -\rho_1(x)t, \tag{3.6}$$

$\phi_{1,2,3}(t = 0) = 0$, which tells us that there is a time dependent driver capable of affecting coherence when the linear frequencies $v_{g_p}\kappa_j$ are re-inserted into the left-hand sides of (2.7)–(2.9) as mentioned earlier.

We now analyze mode dynamics in the Fourier space to see if it indeed displays coherence when frequency broadening is absent; we insist that up to this point we have no guarantee that coherent behavior is actually present. Take for instance modes in the first comb. We shall examine how a mode a_{1j} with wave vector κ_j moves under the action of the driver force-field formed by a_2 and a_3. The expression for a_{1j} can be written in the form

$$a_{1j}(t) = \frac{1}{L}\int a_1(x,t)e^{-i\kappa_j x}\,dx = \frac{1}{L}\int \rho_1(x)\exp[i(-2\rho_1(x)t - \kappa_j x)]\,dx, \tag{3.7}$$

which can be converted into the form

$$a_{1j}(t) = i\frac{1}{2L}\partial_t \int \exp[-i(2\rho_1(x)t + \kappa_j x)]\,dx. \tag{3.8}$$

The evaluation of a_{p_j} thus involves integrals of the form $I = \int e^{i\psi(x)}\,dx$, which can be approximately calculated with help of saddle point (or stationary-phase) methods: $I \sim e^{i\psi(x_0)}\sqrt{2\pi i/\psi''}$, where x_0 is such that $\psi'(x_0) = 0$, primes indicating space derivatives. Translating these rules to our problem yields

$$a_{1j} \sim e^{i3\pi/4}\frac{\sqrt{\pi}}{2L}\frac{d}{dt}\left[\frac{e^{-i[2\rho_1(x_0)t + \kappa_j x_0]}}{\sqrt{-\rho_1''(x_0)t}}\right], \tag{3.9}$$

where the coordinate x_0 of the saddle point is to be determined from

$$2\rho_1'(x_0)t = -\kappa_j. \tag{3.10}$$

In terms of wave packets, for most of the applications curve a_{p_j} *versus* κ_j displays a bell-shaped format with maximum at $\kappa_j = 0$. The curve $\rho_p = \rho_p(x)$ is likewise typically bell-shaped which we assume to be centered at $x = 0$, with the absolute value of the derivatives ρ_p' presenting a maximum on each side of the origin. In the case of comb '1', at any time satisfying $t > t_j \equiv |\kappa_j|/(2|\rho_1'|_{\max})$ the wave vector κ_j

satisfies the saddle condition for some x_0. Then, as time grows, the saddle point moves towards $x_0 \to 0$ such that $\rho_1' \to 0$ and the asymptotic form for mode a_{1j} becomes

$$a_{1j} \sim \rho_1(0)\frac{\sqrt{\pi}}{L}\frac{e^{-i[2\rho_1(0)t-\pi/4]}}{\sqrt{|\rho_1''(0)|t}} \equiv a_{\text{analytical}} \quad (\rho_1''(0) = -|\rho_1''(0)|) \tag{3.11}$$

which suggests that all modes tend to vibrate similarly in asymptotic regimes, under the action of a single nonlinear frequency

$$\Omega_{\text{nl}} \equiv -2\rho_1(0). \tag{3.12}$$

We point out that $a_{\text{analytical}}$ does not depend on the mode index. Given the bell-shaped curve for $\rho_1'(x)$, there are two other saddle points approaching $x_0 \to \pm\infty$, but both can be discarded in view of the fact that the corresponding amplitudes, proportional to ρ_1 or its derivatives, vanish.

The important saddle property analyzed above indicates that as long as linear broadening remains not significant, phase-locking involving the modes prevails, and this represents the same kind of dynamics seen in previous papers (Robinson and Drysdale 1996; de Oliveira et al. 2002). As a matter of fact, and now looking at the problem from the perspective of a test mode calculation, given continuity we expect to observe phase-locking even if a narrow broadening is added to the right-hand sides of (3.1)–(3.3). Phase-locking would be expected to be operative while in terms of absolute value the nonlinear frequency Ω_{nl} stays much larger than the linear frequency $v_{g_1}\kappa_j$ of the largest active test mode j (Robinson and Drysdale 1996; de Oliveira et al. 2002). On the other hand, if the resonance condition

$$\Omega_{\text{nl}} = -v_{g_1}\kappa_{\text{r}}, \tag{3.13}$$

is met for a resonant mode κ_{r}, unlocking and incoherence are expected to set in. We conclude that the overall dynamics are likely to develop essentially along the following possible lines.

(i) None of the original modes meets the resonant criterium initially. In this case, one would first see a gradual inclusion of modes into the overall dynamics according to the linear rule (3.10) derived earlier

$$\kappa = \pm 2|\rho_1'|_{\max}t. \tag{3.14}$$

If dissipation and dispersion—the latter being represented by higher order space derivatives—are ignored as we do in the present analysis, wave vector spread would proceed until such a time when a resonant mode κ_{r} satisfying the resonant condition (3.13) is excited. Then the mode would grow independently and coherence would be lost. From the perspective of test mode calculations, one has an approximate equation for a test mode ${a_1}_j^{\text{T}}$:

$$i\dot{{a_1}_j^{\text{T}}} = v_{g_1}\kappa_j {a_1}_j^{\text{T}} + (a_2^{(0)}a_3^{(0)})_{\kappa_j}. \tag{3.15}$$

The nonlinear source is calculated under the approximation $v_{g_1} = 0$, and $v_{g_2} = v_{g_3} = 0$ is assumed. If one subtracts from (3.15) the corresponding equation with broadening suppressed, one obtains

$$i\delta\dot{a}_{1j} = v_{g_1}\kappa_j \delta a_{1j} + v_{g_1}\kappa_j {a_1}_j^{(0)}, \tag{3.16}$$

with $\delta a_{1j} \equiv {a_1}_j^{\text{T}} - {a_1}_j^{(0)}$. When the source frequency becomes equal to the linear

frequency of the oscillator described by (3.15) at a resonance $j = r$, one can use a slow modulational approach and write $\delta a_{1\mathrm{r}} = \widetilde{\delta a_{1\mathrm{r}}} \exp(-iv_{\mathrm{g}_1}\kappa_{\mathrm{r}}t)$ to obtain $\dot{\widetilde{\delta a_{1\mathrm{r}}}} \sim v_{\mathrm{g}_1}\kappa_{\mathrm{r}}\widetilde{a_{1\mathrm{r}}^{(0)}}$ with the oscillatory factor factored out of the source which therefore grows monotonically for a short period of time after it is excited. One thus sees that the amplitude of the resonant mode, once excited, accompanies the source, growing monotonically. This growth arrests when the collective dynamics departs appreciably from the coherent behavior seen in the previous case. Of course, if field amplitudes are such that the resonant wave vector κ_{r} is larger either than the dissipative or dispersive scales, coherence is likely to be preserved throughout the dynamics because dissipation and dispersion may arrest the spread.

(ii) One of the originally present modes already satisfies the resonance condition (3.13). In this case there is in fact no coherent dynamics at all, even for small times, and this is the case classified as incoherent in previous works (Robinson and Drysdale 1996; de Oliveira et al. 2002).

As a final issue, we observe the following. In the regime where the resonant wave vector κ_{r} lies outside the initial spectral distribution used to construct functions $a_p(x, t = 0)$, coherence time approximately coincides with the transit time of the first comb relative to the others. Indeed, the resonant time t_{r} can be written from expressions (3.13) and (3.14), as mentioned above, in the form $t_{\mathrm{r}} = |\kappa_{\mathrm{r}}|/|2\rho_1'|_{\max} \sim (\rho_0/v_{\mathrm{g}_1})/(\rho_0/d) = d/v_{\mathrm{g}_1}$ which means $v_{\mathrm{g}_1}t_{\mathrm{r}} \sim d$, indicating that as resonance is approached, the first comb moves away from the interaction region.

All the previous comments of course only form a rough theoretical view of the problem and must be supplemented with the appropriate numerical analysis. This is our next task where we focus on case (i); case (ii) can be obtained as the appropriate limit when the resonant wave vector κ_{r} is very small.

4. Wave simulations

We now proceed to simulations of the complete wave set described by (2.10)–(2.12). Simulations are done with a pseudo-spectral method involving $N = 2^{15}$ modes. In all runs we take $v_{\mathrm{g}_2} = v_{\mathrm{g}_3} = 0$. In other words, we assume that the group velocities of combs '2' and '3' are the same, and that we are working in the reference frame where both velocities vanish. This only means that we have made a transformation of variables of the type leading to set (2.10)–(2.12) where $t \to t$ and $x - v_{\mathrm{g}}\, t \to x$, v_{g} now representing either v_{g_2} or v_{g_3}. In this case v_{g_1} represents the group velocity of the first comb *relative* to the other two and this suffices for our analysis. The theory, either in the transformed or original variables, produces the same physical results. In addition to that, we take the following initial conditions for our combs in the space–time representation

$$a_1(x, 0) = \rho_0 e^{-x^2/d^2}, \quad a_{(2,3)}(x, 0) = \sqrt{2}\rho_0 e^{-x^2/d^2}. \tag{4.1}$$

From that we obtain the initial spectral distribution $a_{p_j} = 1/L \int a_p(x) e^{-i\kappa_j x}\, dx$ used in the simulations, which can be approximately written as

$$a_{1\,j} = \sqrt{\pi}\rho_0 \left(\frac{d}{L}\right) e^{-\kappa_j^2 d^2/4}, \quad a_{(2,3)\,j} = \sqrt{2\pi}\rho_0 \left(\frac{d}{L}\right) e^{-\kappa_j^2 d^2/4} \tag{4.2}$$

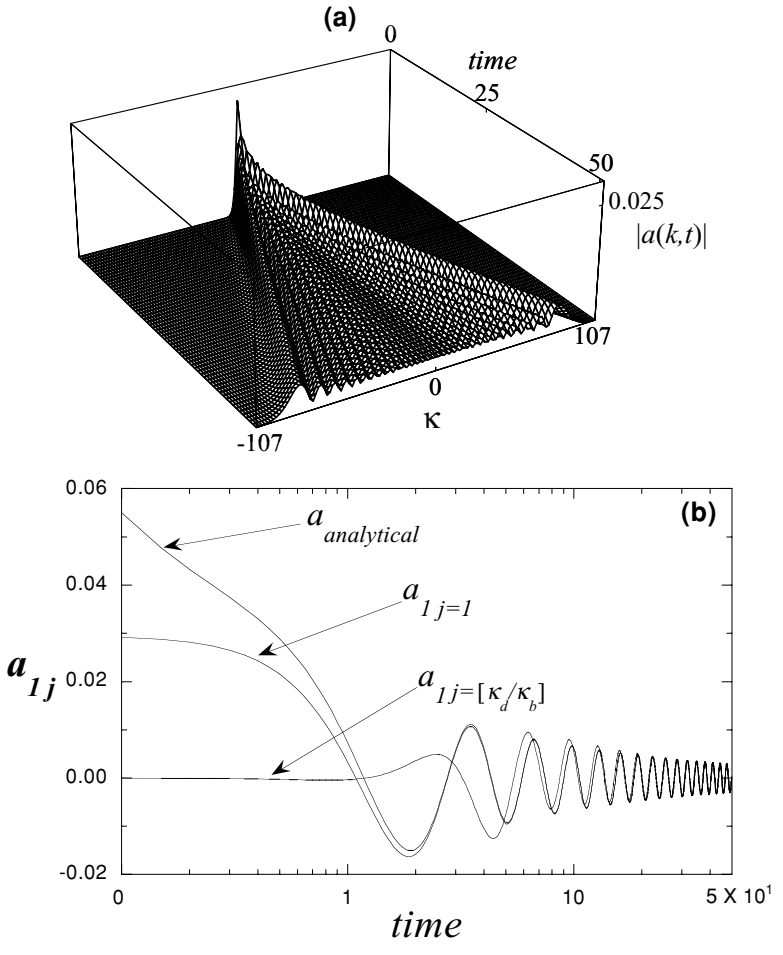

Figure 1. (a) Wave vector spread as a function of time. (b) Comparison of the analytical model $a_{\text{analytical}}$ and mode simulations, with all modes progressing to phase-locking. $v_{g_1} = 0$ in both cases with other parameters as listed in the text.

if $L \gg d$; in all numerical runs we take $L/60 = d = \rho_0 = 1$. From (4.1), the nonlinear frequency (3.12) is estimated as $-2\rho_0$ and from (4.2) the initial extreme linear frequencies of the comb are estimated as $\pm v_{g_1} 2\pi/d$, corresponding to the extreme wave vectors $\pm\kappa_d \equiv \pm 2\pi/d$ contained in the original spectrum at $t = 0$. Let us start with the case where v_{g_1} is set to zero. This is the situation where the linear frequency broadening is absent and is the crucial case to test our ideas on phase-locking and coherence. One way to investigate the issue is to produce a three-dimensional plot of the amplitudes $|a_{1\,j}|$ *versus* time and wave vector κ. This is shown in Fig. 1(a), where we readily see wave vector spread as a function of time as predicted by our saddle point calculations. The spread is linear, following the law $\kappa \sim \pm 2(\rho_0/d)t$. Not only that, but the spread also displays the decay feature represented by our numerical factor $(|\rho_1''(x=0)|t)^{-1/2}$ observed in expression (3.11). That coherence gradually dominates the dynamics can be observed in Fig. 1(b), where we compare the dynamics of the real part of the function $a_{\text{analytical}}$ calculated

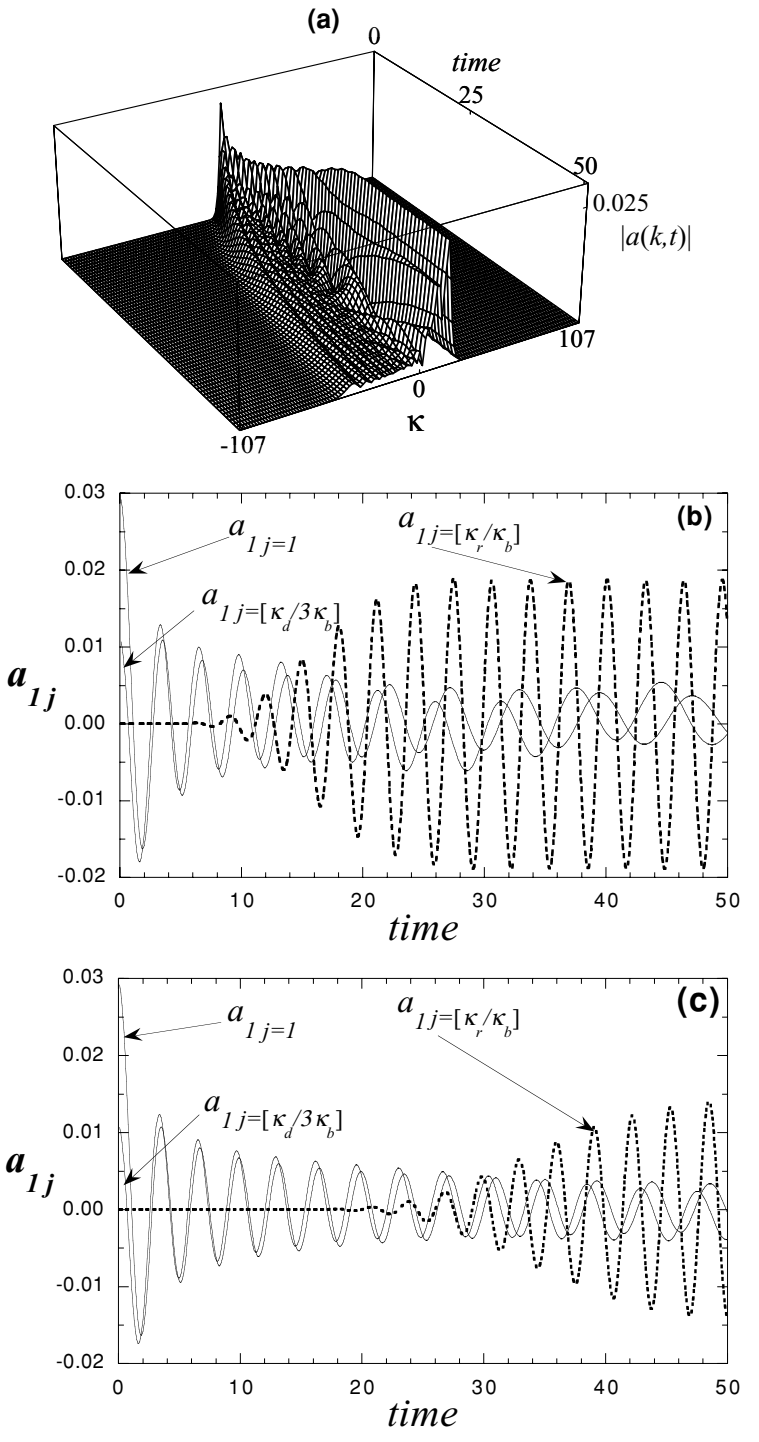

Figure 2. (a) Resonance interrupting regular wave vector spread, $v_{g_1} = 0.1$. (b) and (c) Resonance effects destroying phase-locking of modes, $v_{g_1} = 0.1$ in (b) and $v_{g_1} = 0.05$ in (c). Other parameters as listed in the text.

earlier with the simulated modes $a_{1j=1}$, $a_{1j=[\kappa_d/\kappa_b]}$, where $[\cdot]$ denotes *integer part* and $\kappa_b \equiv 2\pi/L = 2\Delta/N$ is the basic wave vector of the system. Even with both simulated modes starting from distinct initial conditions as a result of the considerable difference of mode indexes (the second mode sits at the border of the original group of wave vectors), the dynamics become asymptotically the same, tending to $a_{\text{analytical}}$. As time evolves, more and more modes become involved, all progressing to the same predicted oscillatory regime. With the insertion of a small linear broadening represented by a group velocity v_{g_1}, the time history undergoes the changes anticipated before. If one takes $v_{g_1} = 0.1$, then $\kappa_r \approx 20$ and the time to attain resonance is $t_r \sim 10$. Fig. 2(a) displays the three-dimensional plot $|a_{1j}(t)|$, similar to Fig. 1(a), but now for $v_{g_1} = 0.1$. One clearly sees that the previous symmetric aspect of Fig. 1(a) is changed. Modes with positive κ are more strongly excited than modes with negative values of this quantity, due to signs of Ω_{nl} and (3.13). By the time one reaches and advances beyond the resonant time t_r, the three-dimensional plot becomes heavily changed if compared with that plot in Fig. 1(a). We point out that after resonant modes are excited, wave vector spread ceases, which is a result of the relative drift of the combs as observed earlier. The wave vector distribution is, however, only slightly affected by resonant effects while $t \ll t_r$, according to all predictions. To complement the information contained in Fig. 2(a), in Fig. 2(b) we depict the real part of modes $a_{1j=1}$, $a_{1j=[\kappa_d/3\kappa_b]}$ and $a_{1j=[\kappa_r/\kappa_b]}$. Apart from the $j = 1$ mode and the resonant mode κ_r, we choose a more internal mode $\kappa = \kappa_d/3$ than the border $\kappa = \kappa_d$ represented in Fig. 1(b) to make the locking–unlocking feature clear. Indeed it is not difficult to appreciate the linear growth of the resonant mode, and that phase-locking and coherence are lost when the resonant mode is strongly excited. For small times prior to resonance all modes tend to phase-lock, but the process is broken when resonant effects start to take over. The same kind of analysis is repeated for $v_{g_1} = 0.05$ in Fig. 2(c), where the resonant mode is now the one associated with this new group velocity. It is seen that unlocking and resonance are both twice as delayed as in the case of the larger group velocity. It is still worth mentioning that this locking–unlocking kind of behavior is radically different from linear systems where modes never tend to locking states; in linear cases with frequency broadening, phase slippage is always present at any time.

5. Conclusions

In this paper we have analyzed microscopic details of the transition from coherence to incoherence in nonlinear wave systems. We have extended previous results to examine models where nonlinear terms must satisfy selection rules. Specifically, we demand wave vector selection rules, which are not considered in earlier works, and find that the basic features are somewhat similar to those models where selection rules are absent: if the nonlinear frequencies are much larger than the linear frequencies of the involved modes, phase-locking is present and the dynamics are coherent. On the other hand, when the linear frequencies become of the same order of magnitude as the nonlinear frequency, phase-locking ceases and the transition to incoherence may be observed. In contrast to previous models, however, wave spread is present and gradually involves a larger and larger number of modes. Whilst frequency broadening is much smaller than field amplitudes, the dynamics are coherent, but transition to incoherence is to be expected when the resonant

mode is excited at $t_r \sim d/v_g$ as calculated before. We expect that terms left aside from our analysis, as dispersive terms, may be responsible for arresting wave vector spread. At the present point we do not have a precise answer regarding this issue, but if dispersion actually arrests the spread it might eventually produce a compact packet of coherent wave modes exactly as in the unrestricted case.

Acknowledgements

This work was partially supported by Conselho Nacional de Desenvolvimento Científico, CNPq, Brasil.

References

Ablowitz, M. J. and Segur, H. 1981 *Solitons and the Inverse Scattering Transform*. SIAM.

Chian, A. C.-L. and Alves, M. V. 1988 *Astrophys. J.* **330**, L77.

de Oliveira, G. I., Frichembruder, M. and Rizzato, F. B. 2002 *Physica* D **164**, 59.

Drysdale, P. M. and Robinson, P. A. 2002 *Phys. Plasmas* **9**, 4896.

Frichembruder, M., Pakter, R., Gerhardt, G. and Rizzato, F. B. 2000 *Phys. Rev.* E **62**, 7861.

Gratton, F. T., Gnavi, G., Galvão, R. M. O. and Gomberoff, L. 1997 *Phys. Rev.* E **55**, 3381.

Kivshar, Y. S. and Malomed, B. 1989 *Rev. Mod. Phys.* **61**, 763.

Martins, A. M. and Mendonça, J. T. 1988 *Phys. Fluids* **31**, 3286.

Rizzato, F. B., Pakter, R. and Lopes, S. R. 2003 *Phys. Rev. E* **68**, 056601.

Robinson, P. A. and Drysdale, P. M. 1996 *Phys. Rev. Lett.* **77**, 2698.

Sagdeev, R. Z. and Galeev, A. A. 1969 *Nonlinear Plasma Theory*. New York: W. A. Benjamin.

Shukla, P. K., Rao, N. N., Yu, M. Y. and Tsintsadze, N. L. 1986 *Phys. Letts.* **138**, 1.

Thornhill, S. G. and ter Haar, D. 1978 *Phys. Reports* **43**, 43.

Weiland, J. and Wilhelmsson, H. 1977 *Coherent Non-Linear Interaction of Waves in Plasmas*. Oxford: Pergamon Press.

Wong, A. Y. and Quon, B. H. 1975 *Phys. Rev.* A **34**, 1499.

Zakharov, V. E., Musher, S. L. and Rubenchik, A. M. 1985 *Phys. Rep.* **129**, 285.